ChemPubSoc Europe

DOI: 10.1002/cctc.201901827

CHEMCATCHEM Full Papers

Targeted Enzyme Engineering Unveiled Unexpected Patterns of Halogenase Stabilization

Hannah Minges,[a] Christian Schnepel,[a] Dominique Böttcher,[b] Martin S. Weiß,[b] Jens Sproß,[c] Uwe T. Bornscheuer,[b] and Norbert Sewald*[a]

Halogenases are valuable biocatalysts for selective C–H activation, but despite recent efforts to broaden their application scope by means of protein engineering, improvement of thermostability and catalytic efficiency is still desired. A directed evolution campaign aimed at generating a thermostable flavin-dependent tryptophan 6-halogenase with reasonable activity suitable for chemoenzymatic purposes. These characteristics were tackled by combining successive rounds of epPCR along with semi-rational mutagenesis leading to a triple mutant (Thal-GLV) with substantially increased thermostability ($\triangle T_M = 23.5$ K) and higher activity at 25 °C than the wild type enzyme. Moreover, an active-site mutation has a striking impact on thermostability but also on enantioselectivity. Our data contribute to a detailed understanding of biohalogenation and provide a profound basis for future engineering strategies to facilitate chemoenzymatic application of these attractive biocatalysts.

Introduction

Synthetic functionalization of non-activated C–H moieties usually requires noble metal catalysts, toxic reagents, or extreme conditions, generating considerable amounts of undesired by-products and waste. Engineering new enzymes via directed evolution as a shortcut of Darwinian evolution by combining random mutagenesis with a suitable selection process is appreciated as a promising approach to replace synthetic catalysts and to improve reaction pathways suffering from low sustainability. Evolved enzymes can be generated at comparatively low cost and their incorporation into metabolic pathways paves the way to develop cellular factories dedicated to selective fine chemical production.[1,2] In ground-breaking evolution campaigns it was demonstrated by Arnold *et al.* that tailor-made enzymes could be generated to catalyze new-to-nature reactions like cyclopropanation or aziridination using engineered monooxygenases.[3,4] Intrigued by the power of evolution and recognizing an increasing demand for selective C–H activation catalysts we felt encouraged to improve halogenase performance by means of protein engineering to qualify for their application in biotechnology.

The synthetic interest in halogenated compounds lies in their ability to act as building blocks and starting material for further modifications, particularly as they provide access to a large range of valuable products for metal catalyzed cross-coupling reactions. In pharmaceutical and agrochemical chemistry halogenation often confers unique biological activities that qualifies this synthetic methodology as an indispensable tool in synthetic chemistry.[5,6] As more than 5000 organohalogen compounds are known from terrestrial and marine organisms, it seems obvious to study and improve the elaborate repertoire of halogenating enzymes.[7] In general, the introduction of halogens into organic scaffolds can be carried out on aliphatic carbons, olefins as well as aromatic and heterocyclic rings.[8] Electrophilic aromatic substitution is a widely-applied reaction type for arene functionalization that is of major importance for the synthesis of bulk and fine chemicals. However, an immense obstacle is that conventional approaches for the introduction of halogens require harsh conditions, while addressing electronically unfavored positions remains challenging. As a consequence, mixtures of regioisomers may be obtained resulting in a low overall yield of the desired product, undesired by-products and hazardous waste.[9] Conversely, enzymatic halogenation provides a safe alternative for the synthesis of haloarenes enabling the regioselective halogenation of organic scaffolds under benign reaction conditions. Among the halogenating enzymes, flavin-dependent halogenases currently provide the best candidates with regard to chemoenzymatic utility. These biocatalysts merely require a

[a] H. Minges, Dr. C. Schnepel, Prof. Dr. N. Sewald
Organic and Bioorganic Chemistry
Department of Chemistry
Bielefeld University
Universitätsstraße 25
33615 Bielefeld (Germany)
E-mail: norbert.sewald@uni-bielefeld.de
[b] Dr. D. Böttcher, Dr. M. S. Weiß, Prof. U. T. Bornscheuer
Institute of Biochemistry
Department of Biotechnology and Enzyme Catalysis
Greifswald University
Felix-Hausdorff-Str.4
17489 Greifswald (Germany)
[c] Dr. J. Sproß
Industrial Organic Chemistry and Biotechnology
Department of Chemistry
Bielefeld University
Universitätsstraße 25
33615 Bielefeld (Germany)

Supporting information for this article is available on the WWW under https://doi.org/10.1002/cctc.201901827

This publication is part of a joint Special Collection with ChemBioChem on "Excellence in Biocatalysis Research". Please follow the link for more articles in the collection.

halide salt, molecular oxygen, and $FADH_2$ as stoichiometric components. Owing to their convenient handling at room temperature and pH 7.4 without needing activating or protecting groups, enzymatic halogenation emerged as a versatile tool for organic chemistry, as it may help to overcome drawbacks of chemical halogenation.[10] Tryptophan halogenases hitherto constitute the most examined members of this class, as they catalyze halogenation of L-tryptophan as a free substrate, not requiring any carrier protein. Regeneration of the cofactor is achieved *in situ* with the NADH-dependent flavin reductase PrnF and, conversely, NADH regeneration with an alcohol dehydrogenase or any other enzyme catalyzing NAD^+ reduction (Scheme 1).[11]

In 2000 van Pée and coworkers isolated and characterized PrnA, the first member of the tryptophan halogenase family, from *Pseudomonas fluorescens*.[12] Further FAD-dependent tryptophan halogenases, such as the Trp 7-halogenase RebH from *Lechevalieria aerocolonigenes*,[13] the Trp 6-halogenase Thal from *Streptomyces albogriseolus*,[14] and the Trp 5-halogenase PyrH from *Streptomyces rugosporus*[15] were identified and characterized as biocatalysts.[16,17]

Enzymatic halogenation introduces a hotspot for further one-pot aryl functionalization in chemocatalytic transformations. Therefore, we and other groups sought to combine biotransformations such as enzymatic halogenation with Suzuki-Miyaura cross-coupling.[18–21] As disclosed in a publication by the Gröger group, one-pot feasibility of a Pd/Cu-catalyzed Wacker oxidation and an enzymatic ketone reduction was achieved via compartmentalization of the reactions employing a polydimethylsiloxane (PDMS) thimble.[22] Based on these findings, Micklefield *et al.* contributed progress on the combination of biohalogenation and chemocatalysis into a sequential one-pot process. Here, membrane compartmentalization enabled the combination of FAD-dependent halogenases with palladium-catalyzed cross-coupling in a one-pot manner.[23] Recently Goss *et al.* developed an *in vivo* approach for the generation of a brominated natural product analogue and its subsequent cross-coupling for diversification of halogenated natural products however, without mentioning turnover or efficiency.[24] Despite substantial efforts to improve *in vitro* compatibility of halogenases, their application still suffers from severe shortcomings such as low activity, enzyme stability and their limitation to act on relatively electron rich aromatic compounds.

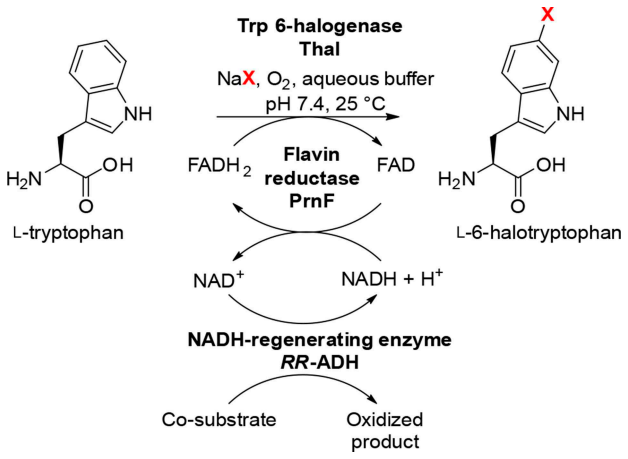

Scheme 1. Thal-catalyzed halogenation of L-tryptophan leading to chlorination or bromination at the C6-position of the indole moiety at pH 7.4 and 25 °C. The cofactor $FADH_2$ is regenerated by the flavin reductase PrnF and NADH is provided by an alcohol dehydrogenase (*RR*-ADH) or another enzyme component. X = Cl, Br

Engineering of Halogenases

Several approaches have been developed in recent years to overcome limitations of tryptophan halogenases by means of directed evolution. A comprehensive survey by Lewis *et al.* focused on profiling of the substrate spectrum of several FAD-dependent halogenases towards a broad set of arenes with different steric and functional groups. Examination of substrate-activity profiles revealed that the substrate scope of FAD-dependent halogenases is less strict than previously assumed. Moreover, the study unveiled that notable differences of the substrate profile exist among these enzymes despite high homology.[25] Studies by Andorfer *et al.* demonstrated that the regioselectivity of the tryptophan 7-halogenase RebH could be altered by combining random and targeted mutagenesis. Aiming to engineer RebH into a C5- or C6-regioselective biocatalyst led to the generation of two new complementary halogenase variants, catalyzing the chlorination of tryptamine with high regioselectivity for positions C5 and C6, respectively.[26] Based on the active site of Trp 7-halogenase PrnA van Pée's group generated a single mutant with relaxed regioselectivity, yielding a 2:1 mixture of 5- and 7-brominated Trp.[27] Recently, structure-based protein engineering performed by Moritzer *et al.* enabled a pronounced alteration of regioselectivity that was exemplified for the Trp 6-halogenase Thal. Exchange of merely five active-site residues of Thal into the corresponding counterparts of RebH generated a quintuple variant exhibiting a nearly complete switch from C6- to C7-halogenation with $>95\%$ selectivity.[28]

Engineering Towards Increased Thermostability

Multiple examples of thermal enzyme stabilization obtained by directed evolution are reported in literature. Kitaoka *et al.* achieved an impressive improvement in thermostability of a phosphorylase from *Bifidobacterium longum* JM1217 by creating a double mutant exhibiting a 20 °C higher thermostability than the wild type that paved the way to an industrial process for oligosaccharide production.[29] Even though, several studies are reported where increased thermostability was not detrimental to enzyme activity,[30,31] in a series of evolution campaigns targeting increased thermostability, decreased catalytic efficiency of the thermostable variants was noted.[32–34] For instance, a thermostable amylase mutant from *Thermus* sp. strain IM6501 (ThMA) containing seven individual mutations resulted in a 15 °C increase of the optimal reaction temperature.

Still, this significant gain in thermostability was achieved at the expense of decreased enzyme activity due to introduction of mutation M376T.[34] Likewise, Singh and coworkers performed a directed evolution campaign to improve the thermostability of a xylanase (XynA) from *Thermomyces lanuginosus*. Evolving a biocatalyst suitable for harsh conditions of an industrial application revealed a compromise between stability and activity for most of the obtained mutants.[35] Recent efforts also focused on improving the thermostability of Trp halogenases. As reported by Poor *et al.*, three rounds of mutagenesis resulted in a thermostable RebH variant containing eight randomly introduced mutations leading to an increased melting temperature of 18 K. In addition to an increased conversion of tryptophan, improved conversion was also detectable for unnatural substrates. However, despite these improvements its catalytic efficiency was reduced.[36] In general, low activity towards substrates and notable instability cannot be neglected, as these deficiencies hinder an application in industrial processes. Thermostable enzymes serve as promising starting points for further engineering amenable to address other enzyme properties as these biocatalysts often show a higher tolerance towards random mutations.[37] Due to a current lack of elaborate engineering campaigns on stabilizing Trp halogenases, we aimed at modifying and optimizing the tryptophan 6-halogenase Thal. Particularly, we embarked on unveiling crucial motifs to improve halogenase performance in order to obtain a catalyst with increased thermostability and activity at elevated temperatures.

Results and Discussion

Identification of Thermostable Thal Variants Applying a High-Throughput Fluorescence Assay

A quantitative halogenase high-throughput fluorescence assay applicable in microtiter plates, previously developed by us, served to reduce the screening effort of large mutant libraries.[38] This robust halogenase screening method utilizes Suzuki-Miyaura cross-coupling (SMC) with a fluorescence readout enabling screening in cell lysate. Among a range of arylboronic acids tested *a priori*, coupling between 3-aminophenylboronic acid and the brominated amino acid turned out to be most efficient to monitor quantitative formation of bromotryptophan due to superior fluorescence properties. This activity assay in combination with a high-throughput strategy previously enabled identification of the thermostable variant Thal-GR comprising mutations S359G/K374R, which exhibits a significantly increased thermostability and 2.5-fold improved activity.[38]

Based on prior achievements obtained from the first round of Thal evolution we now embarked on a more comprehensive evolution campaign to further improve its thermostability and activity. Fluorogenic high-throughput screening previously established served to identify improved halogenases from random mutant libraries.

Starting from a modified evolution procedure, libraries of Thal-GR mutants were constructed via epPCR and MEGAWHOP cloning. Promising variants exhibiting increased thermostability were subsequently detected by fluorogenic cross-coupling (Figure 1). For this purpose, the mutated Thal-GR colonies were picked and cultivated in microtiter plates for halogenase expression and screening. Upon lysis, the libraries were treated for 20 min at 59 °C to select variants with enhanced thermostability. The Thal-GR template served as a reference and possessed significantly decreased activity under these screening conditions providing selection pressure for enhanced thermostability.

With this setup in hand, high-throughput screening via SMC to monitor residual conversion of tryptophan revealed the beneficial mutation I393V (Thal-GRV). To confirm increased enzyme stability, purified protein samples of Thal-GRV were incubated between 47.0 and 67.0 °C for 20 min and subsequently assayed for bromination activity at 25 °C. Determination of the half-maximal conversion temperature (T_{50}) from these data revealed an increase of 1.1 K compared to Thal-GR. Likewise, the melting point (T_M) determined by nanoDSF was increased to 1.8 K that is 18 K higher than the parameters of wild type protein (Table 1, Figure 2A).

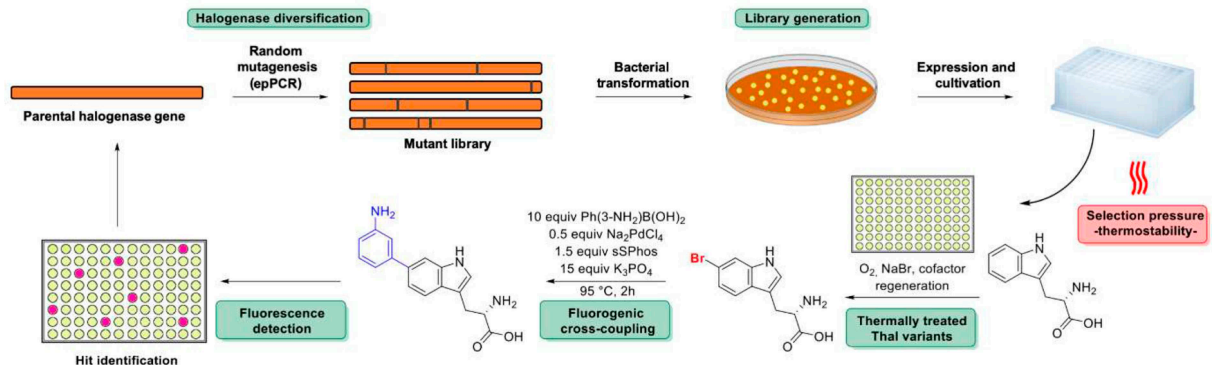

Figure 1. High-throughput halogenase engineering assay based on Suzuki-Miyaura cross-coupling (SMC) for the generation of thermostable enzymes. Mutant libraries of the Trp 6-halogenase Thal were constructed by epPCR and cultivated and expressed in 96-well plates. After lysis and thermal incubation promising Thal variants were identified by HT-SMC screening for residual bromination activity at 25 °C.

Table 1. Directed evolution of Thal-WT showing the evolved variants and their identified mutations as well as thermostability parameters T_{50} and T_M.

Thal variant	mutation	T_{50} [°C]	T_M [°C]
Thal-WT	–	47.0	47.7
Thal-GR	S359G-K374R	58.6	63.8
Thal-GRV	S359G-K374R-I393V	59.7	65.6
Thal-GLV	S359G-K374L-I393V	63.0	71.2
Thal-GWV	S359G-K374W-I393V	65.5	72.2
Thal-GRV-N	S359G-K374R-I393V-D378N	68.6	n.d.
Thal-GRV-T	S359G-K374R-I393V-A476T	64.3	/
Thal-GRV-MT	S359G-K374R-I393V-L290M-A476T	66.1	n.d.
Thal-GRV-NT	S359G-K374R-I393V-D378N-A476T	70.0	66.0

(n.d. = not determined, / = no reliable data obtained)

Random and Site-Directed Mutagenesis Resulted in Significant Increase of Thermostability

Based on this increased thermostability Thal-GRV served as a template to initiate the third generation of mutants. Screening of merely 176 colonies led to identification of two new variants with significantly higher thermostability, GRV-D378N (Thal GRV-N) with T_{50} = 68.6 °C as well as Thal GRV-L290M/A476T (Thal-GRV-MT) (T_{50} = 66.1 °C). To exclude non-beneficial or detrimental mutations, we investigated whether both residues contributed additively to the elevated thermostability. With the current set of mutations in hand having a putative effect on thermostability we laid our emphasis on evaluation and optimization of residues identified by random evolution. Therefore, the variants Thal-GRV-L290M and Thal-GRV-A476T were generated by site-directed mutagenesis and analyzed as explained above. Interestingly, Thal-GRV-L290M led to a negligible conversion of tryptophan after the heat shock above 66 °C. Thus, this deleterious mutation was rejected from the following evolution campaign. In contrast, Thal-GRV-T confirmed its positive impact on thermostability with T_{50} = 64.3 °C. Both beneficial mutations from the third generation were combined finally providing the considerably more thermostable and robust biocatalyst Thal-GRV-NT. T_{50} increased further reaching 70 °C, whereas the T_M of 66 °C was slightly lower.

Kinetic Characterization Revealed Stability-Activity Trade Off

We wondered whether increased thermostability was evolved at the expense of activity, as had been observed by others.[34,35] For this, specific activities were determined at 25 °C and 40 °C (Figure 2B). To ensure sufficient thermostability of the auxiliary enzyme PrnF responsible for $FADH_2$ supply, its activity at 40 °C was determined. For all Thal variants an increase of activity compared to wild type was observed at 25 °C. At this stage of evolution Thal-GR exhibited highest activity among the variants obtained from random evolution exceeding the wild type by factor two. Interestingly, Thal-GR was also significantly more active than the wild type enzyme both at 25 °C and 40 °C. However, the specific activity decreased again upon further evolution and introduction of additional mutations.

Site-Saturation Mutagenesis for Improving Catalytic Properties

Despite their increased thermostability, the Thal variants identified in the third round of evolution (GRV-N; GRV-T; GRV-MT and GRV-NT) exhibit significantly reduced kinetic performance at elevated temperature. As we wished to retain activity, they were discarded from further evolution. In addition,

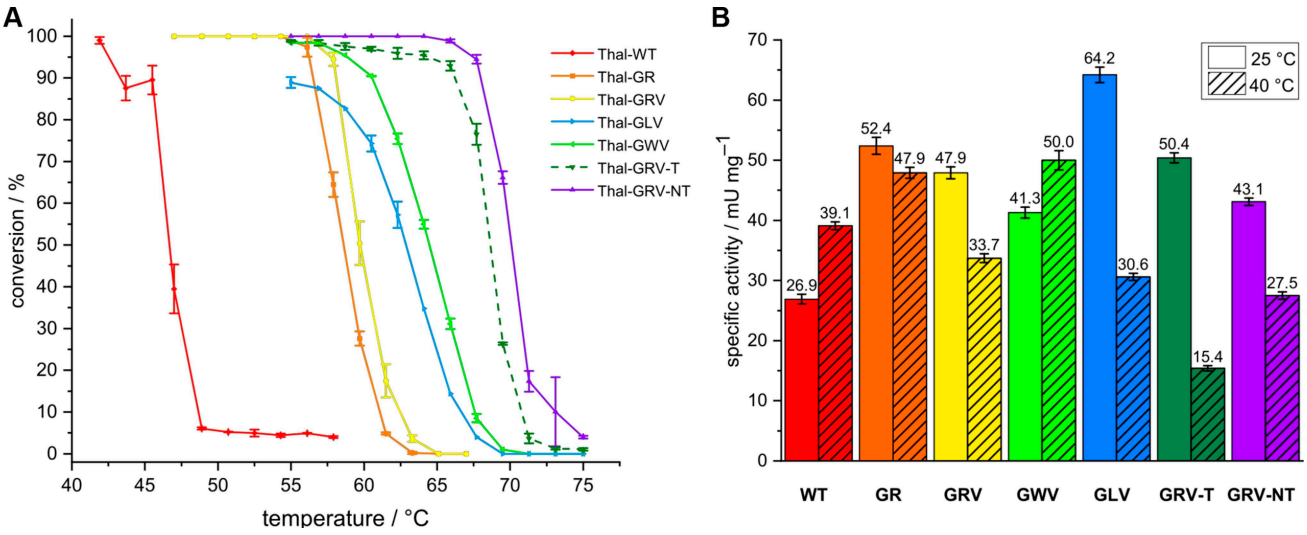

Figure 2. Evolution of thermostability of Thal-WT and determination of catalyst properties. A) Data of half-maximal conversion of L-Trp indicate a stepwise increase in T_{50} during evolution of Thal. Purified halogenase was incubated for 20 min applying a temperature gradient from 42–75 °C. Heat shocked enzyme was employed for bromination of L-Trp at 25 °C. Final conversion of substrate was determined via RP-HPLC in order to calculate T_{50} from sigmoidal regression. B) Determination of specific activity at 25 °C and 40 °C indicated an activity-stability trade-off during evolution of Thal. The subsequently engineered variant Thal-GWV and -GLV exhibited improved thermostability and kinetic parameters compared to Thal-WT.

subsequently identified Thal-GLV mutant exceeded those variants in terms of T_M and specific activity. Among the variants obtained so far, Thal-GRV was considered as the most promising mutant as it combined a significant increase in T_{50} and T_M with elevated specific activity at 25 °C. We deduced that the amino acid positions 359, 374 and 393 proved to be crucial hotspots regarding increased thermostability as well as activity.

Thal-GRV was subjected to site-saturation mutagenesis to further elucidate the impact of the type of amino acid located at these positions. Gly359, Arg374 and Val393 were individually addressed by site-saturation PCR using NNK codon degeneracy to cover the whole set of amino acids. As each of the three addressed amino acids was randomized separately, screening 94 colonies allowed > 95% sequence coverage assuming a negligible wild type background.[39,40] Library quality was verified by Sanger sequencing indicating the desired amino acid bias at the selected position. Mutation of Gly359 or Val393 did not reveal a more thermostable variant, thereby confirming that the previously introduced residues Gly and Val were the most preferred ones. Interestingly, Arg374 seemed to be less beneficial than Leu or Trp in variants Thal-GLV and Thal-GWV. It is worth mentioning that both mutants were identified twice from the Arg374 mutant library.

Taken into consideration that Trp is only encoded by one base triplet, the double identification of this variant is a strong indication for its positive effect on thermostability. Both Thal variants have significantly higher T_{50} values than the wild type enzyme (Thal-GLV: T_{50} = 63.0 °C; Thal-GWV: T_{50} = 65.5 °C) and the melting temperature T_M increased likewise. Since Thal-GWV exceeds the wild type specific activity at 25 °C and 40 °C, this variant turns out to be endowed with substantially improved catalytic properties and the best thermostability parameters obtained during the evolution campaign. Likewise, variant Thal-GLV, also containing a hydrophobic substitution in position 374, exhibits high activity at 25 °C albeit having lower activity at 40 °C compared to Thal-WT. As an elevated optimal reaction temperature (T_{opt}) could be expected for thermostable enzymes, we wondered whether increased thermostability would permit the use of higher reaction temperatures.[36,41,42] Conversion-temperature profiles of Thal-WT and the fittest variants revealed a T_{opt} ranging from 25–30 °C (Figure S2). Hence, T_{opt} was not altered notably despite significantly elevated T_{50} and T_M observed for the evolved variants. However, it should be mentioned that biohalogenation requires an intricate reaction system depending on many influencing factors e.g. cofactor regeneration, oxygen supply etc. Noteworthy T_{opt} determination does not exclusively reflect the characteristics of Thal variants. Even though we ensured that the flavin reductase PrnF remained active after 30 min of incubation at 40 °C and also *RR*-ADH withstands purification via heat-precipitation, it seems probable that auxiliary enzymes and cofactors also suffer from long-term incubation at higher temperatures during the reaction course. Thus, cofactor supply opposes as a drawback of halogenation reactions carried out at higher temperatures. These major bottlenecks should be taken into account when determining optimal reaction temperature of Thal variants. Nevertheless, a long-term stability assay corroborates Thal-GLV's higher robustness and value as biocatalyst. Therefore, Thal-WT and Thal-GLV were incubated at 40 °C for a variable time range and subsequently applied for bromination of L-Trp at 25 °C. As the auxiliary enzymes were added after thermal incubation of halogenase, the concomitant cofactor regeneration should not suffer from any limitation. Accordingly, Thal-GLV withstands 5 h incubation with residual 8% conversion of substrate, whereas the WT enzyme was nearly inactive after 3 h incubation (Table S4).

Hydrophobic Interactions Enhance Enzyme Stability

The power of random evolution especially lies in the identification and localization of unexpected mutations and new hotspots within the protein scaffold that can be hardly predicted by a rational approach. Investigating the location and impact of mutations can support to provide a rationale for increased thermostability. The recently resolved crystal structure of Thal-WT served to localize the mutations known in Thal-GWV-NT.[28,43] As observed for other thermostable enzyme variants such as RebH it was not surprising that the majority of mutations is located on the protein surface remote from the active site (Figure 3).[36] An increase of surface charge is known to impede protein aggregation. Therefore, the elevated thermostability of Thal-GR observed initially could not be deduced from the exchange of Lys374 to Arg374 since both basic residues are capable of forming a salt bridge. Possibly, difference of pK_A values, chain length and conformation of side chains influence interactions to the dimer interface.[44]

As Trp halogenases commonly form homodimers,[45] this Arg residue could favor a salt bridge to the second Thal monomer. Previously Panja *et al.* disclosed that salt bridges occur more frequently in thermophilic proteins, as these contribute to a

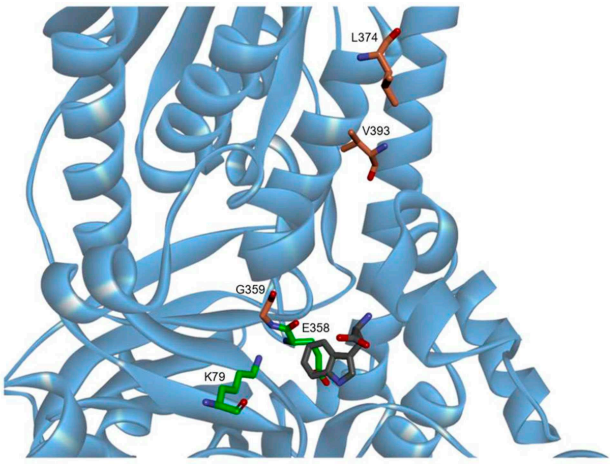

Figure 3. Model of Thal-GLV shown in ribbon format based on the crystal structure of Thal-WT in complex with L-tryptophan (PDB code: 6H44). Residues shown as brown stick model show mutational hotspots derived from evolution of Thal (S359G, K374L, I393V). The conserved amino acid residues K79 and E358 are highlighted as green stick model. The substrate L-Trp is shown in grey. The picture was generated and further modified using Pymol.

more rigid protein scaffold to withstand thermal stress.[46] Surprisingly, site-saturation mutagenesis unveiled that hydrophobic residues are in some cases more favorable for halogenase stability and lifetime. Probably van der Waals interactions and π-stacking support association of the monomers as evident from a Leu or Trp residue at position 374 that was most preferred among all types of amino acids. Similarly, Arnold *et al.* reported that increased stability of an engineered thermostable hydrolase was previously connected to stronger hydrophobic interactions and an increase in hydrophobicity.[30]

Mass Spectrometric Analysis Revealed Increased Tendency for Dimer Formation

MS analysis served to provide insight into the influence of stabilizing mutations on the association of monomers into the corresponding homodimer. Native MS provides a model based on the gas phase that does not exactly reflect the state of the protein in its natural environment. However, it resembles the biological status of the protein in solution, prior to the ionization event, revealing structural information on the protein of interest.[47] Owing to the ability of native ESI-MS to preserve noncovalent interactions, characterization of several protein classes has successfully been applied.[48–50]

It is known from previous reports that tryptophan halogenases PyrH, RebH and PrnA tend to form dimers, as evident from gel filtration and crystal structures.[45,51,52] Likewise, Thal was found as a dimer in the crystal structure whereas it exists as a monomer in solution.[28] ESI-MS measurement performed under native conditions showed that Thal is present in solution both as a homodimer and as a monomer. These findings corroborate that Thal tends to dimer formation in solution similar to other halogenases. When analyzing the mutated isoforms, a higher amount of homodimer in relation to the monomer compared to the wild type enzyme was detected (Figure S4). These data therefore support the hypothesis that elevated thermostability and activity result from increased association of the halogenase monomers. Furthermore, determination of the protein mass by MS under denaturing conditions indirectly confirms the mutation of the targeted amino acids in the Thal variants (Figure S5-S7).

Analysis of Single Mutations Confirmed Significance of Active Site Mutation and Hydrophobic Residues

During each round of Thal evolution the thermostability increased as evident by rise of T_{50} and T_M values. However, selection on improved thermostability does not automatically evolve enzyme activity. As we observed an additive effect on thermostability caused by the mutations D378N and A476T (Thal-GRV-NT), we wished to dissect the individual contribution of each residue to thermostability and catalytic activity. Therefore, single mutants were generated to provide insights on the influence on both parameters.

The serine residue S347 in PrnA is conserved among FAD-dependent tryptophan halogenases and mutation causes severely decreased activity. Even though its role remains elusive yet, S347 was postulated to participate in an extended hydrogen bonding network.[53] Its counterpart S359 in Thal is in close proximity to the essential Glu358, a highly conserved residue among FAD-dependent Trp halogenases postulated to enhance electrophilicity of the halogenating species within the catalytic cycle.[54] We wondered whether the mutation S359G would influence thermostability. Interestingly, the single mutation S359G resulted in a considerably elevated T_{50} exceeding the wild type by more than 7.8 K. This observation was also confirmed by an increase in T_M of 10.9 K, while other single mutations merely led to a slight improvement of the thermostability parameters (Table 2, Figure 4A). Thus, the influence of S359G was probably most decisive even though being located in the active site (Figure 3). Interestingly, the mutation A476T resulted in a less stable biocatalyst, where T_M could not even be determined.

We suggest this mutation to result in decreased enzyme stability associated with denaturation or misfolding. Even though residual activity for Thal-A476T was determined, full conversion of substrate was not achieved in bromination assays. These findings are in line to the reduced specific activity of GRV-T and GRV-NT, finally proving the detrimental effect of mutation A476T (Figure 4B).

Comparison of Enzymatic Parameters and Overall Conversion of Generated Thal Variants

Regarding the specific activity of the Thal single mutants, three mutations (Thal-S359G, Thal-K374W and Thal-I393V) came into focus as they were the only sites significantly exceeding wild type activity at 25 °C as well as at 40 °C. Here, Thal-K374W exhibits the highest specific activity among the single mutants and reaches full conversion of substrate (Figure 5). Like for the WT enzyme full substrate turnover is observed after 60 min. The progress curve reflects that the K374W mutant catalyzes halogenation faster than the WT already reaching >90% conversion after 45 min.

In contrast, Thal-GWV, the most thermostable variant obtained so far, suffers from incomplete conversion and

Table 2. Evolved Thal single mutants to study influence of individual mutations identified by random mutagenesis of Thal with corresponding T_{50} and T_M values.

Thal variant	T_{50} [°C]	T_M [°C]
Thal-WT	47.0	47.7
Thal-S359G	54.8	58.6
Thal-K374R	49.8	48.4
Thal-K374L	51.5	49.7
Thal-K374W	51.1	48.5
Thal-I393V	50.0	46.3
Thal-D378N	51.8	50.0
Thal-A476T	52.0	/

(/ = no reliable data obtained)

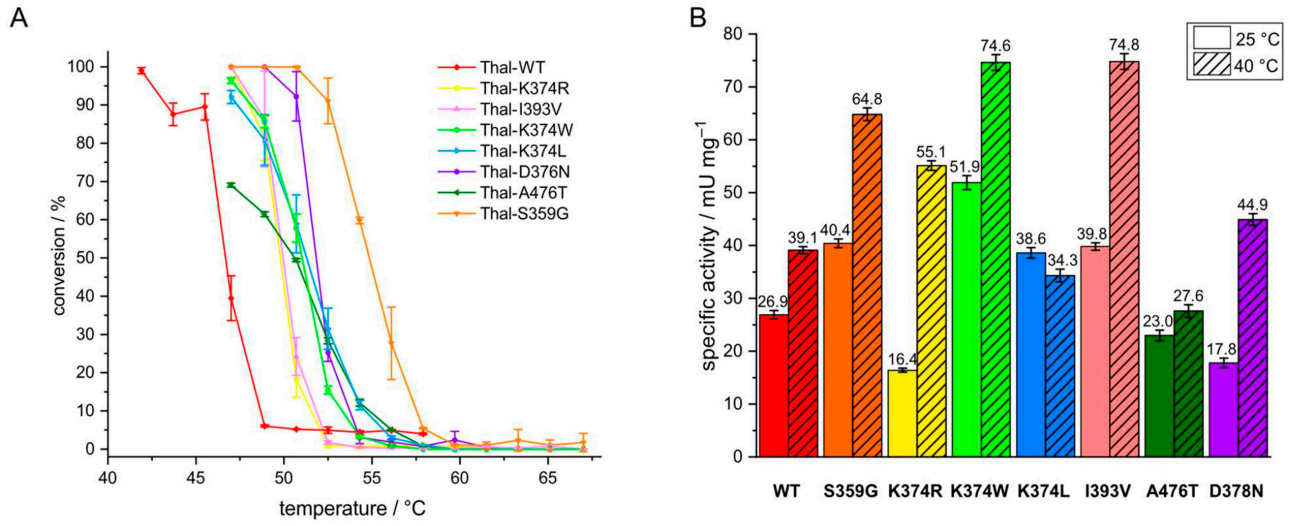

Figure 4. Analysis of thermostability and kinetic parameter for engineered Thal single mutants. A) HPLC-data correlating with the final conversion of L-Trp at 25 °C after incubation of purified halogenase at elevated temperatures for 20 min revealed a significant increase in T_{50} for Thal-S359G. B) Determination of specific activity at 25 °C and 40 °C for Thal single mutants indicated elevated activity of Thal-S359G, -K374W and I393V.

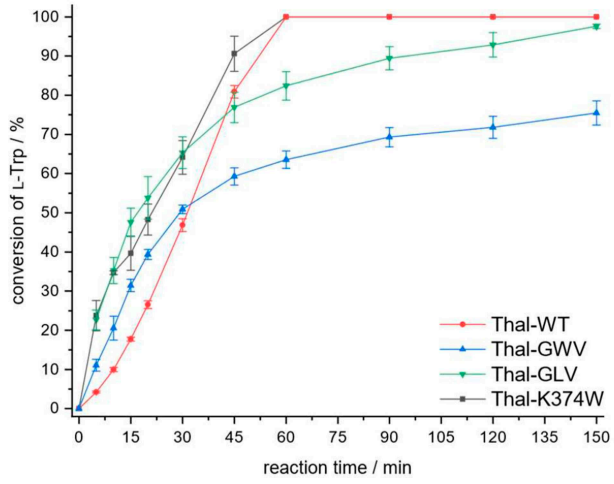

Figure 5. Conversion of L-Trp (1 mM) catalyzed by Thal WT and different variants at 25 °C indicates accelerated conversion compared to WT enzyme. Thal-GWV catalyzed reactions stop at a conversion of 75% whereas all other halogenases reach quantitative substrate turnover. Among all variants Thal-GLV turns out as most valuable biocatalyst whereas Thal-K374W exhibits faster conversion of substrate.

stagnates at 75% bromination of L-Trp. The reason of this deficiency remains elusive until now. Notably, Thal-GLV is endowed with significantly improved T_{50} and T_M and reaches >98% conversion albeit slightly retarded. Concluding from these results, two considerably improved halogenase variants were obtained: Thal-GLV was confirmed as a thermostable biocatalyst with significantly increased halogenation activity also observed at 25 °C. Thal-K374W shows higher activity but less thermostability than GLV.

Further Characterization of Evolved Variant Confirmed Maintained Chlorination Ability but Altered Enantiomer Selectivity

As recently disclosed by Neubauer *et al.*, the FAD-dependent halogenase BrvH, identified from a marine metagenome of *Brevundimonas* sp. BAL3, exhibits a high preference of indole bromination over chlorination. Conversely, Trp halogenases are reported to favor incorporation of less bulky chloride.[15,55] Hence, we examined whether Thal mutagenesis also influences halide selectivity. LC-MS analysis confirmed Thal-GWV's ability to incorporate either chloride or bromide into L-Trp with high efficiency. Hence, mutation S359G did not alter ion selectivity (Figure S8). Though this evolution campaign focusses on increasing thermostability and activity, examples are reported where engineered halogenase variants exhibit improved halogenation of non-natural substrates.[25,36] Most potent variants Thal-GLV and S359G were chosen as representatives to investigate the mutation's effect on a selected panel of different substrates. Both variants show unaffected quantitative conversion of indole and tryptamine, whereas methyl-pyrrole-3-carboxylate was brominated to a lower extent compared to the WT enzyme (Table S5). Apart from L-Trp, Thal also catalyzes the halogenation of D-Trp with comparable high efficiency. It was surprising to observe a substantially lower turnover of D-Trp for the evolved variant Thal-GWV (Table 3). The conversion of D-Trp to D-6-Br-Trp dropped significantly from >99% bromination observed for the wild type to merely 20% for Thal-GWV. It was assumed that the active-site mutation S359G is responsible for this altered preference. Accordingly, the single mutant Thal-S359G is significantly less active towards the D-enantiomer reaching only 17% conversion probably caused by weaker substrate affinity. Likewise, chlorination of D-Trp is also significantly reduced in case of variants harboring mutation S359G. In contrast, conversion of D-Trp is not affected for other

Table 3. Conversion of D-Trp to D-6-Br-Trp by Thal-WT and variants.

Thal variant	Conversion of D-Trp [%]
Thal-WT	>99
Thal-GWV	20
Thal-S359G	17
Thal-K374R	>99
Thal-K374L	>99
Thal-K374W	>99
Thal-I393V	>99
Thal-D378N	>99
Thal-A476T	>99

Reaction conditions: 25 μM Thal variant, 1 mM D-Trp, cofactor regeneration, 3 h at 25 °C.

Thal single mutants described herein, probably because the mutations are located distant to the active site.

To establish the selectivity of the S359G mutant, relative conversion rates of separate bromination reactions of D- and L-Trp were prepared. Applying a lower enzyme loading further reduced conversion of the D-enantiomer that dropped to 3.5% for Thal S359G (Figure 6). However, this mutant revealed steepest conversion of the L-enantiomer compared to Thal-WT. Not surprisingly, the native enzyme exhibited comparable conversion of both enantiomers, whereas a slight preference for the native substrate L-Trp was noted. In addition, a competition experiment applying a mixture of L- and D-tryptophan in a ratio of 1:1 was carried out to provide unambiguous insight into altered enantiomer preference. After incubation for 24 h at 25 °C Marfey's derivatization of reaction mixtures combined with LC-MS analysis permitted separation of resulting diastereomers comprising either D-/L-Trp or D-/L-6-Br-Trp. The expected diastereomer signals formed upon coupling with N^{α}-(2,4-dinitro-5-fluorophenyl)-L-alaninamide (FDAA) were identified by LC-MS and comparison with authentic standards. Thal-WT exhibited complete conversion of both enantiomers as evident from two signals ascribed to the L- and D-6-Br-Trp-containing diastereomers. In contrast, Thal-S359G's strong preference for L-Trp was evident from its quantitative conversion to L-6-Br-Trp, whereas the D-configured substrate enantiomer was not converted and accumulated in the reaction mixture (Figure S9).

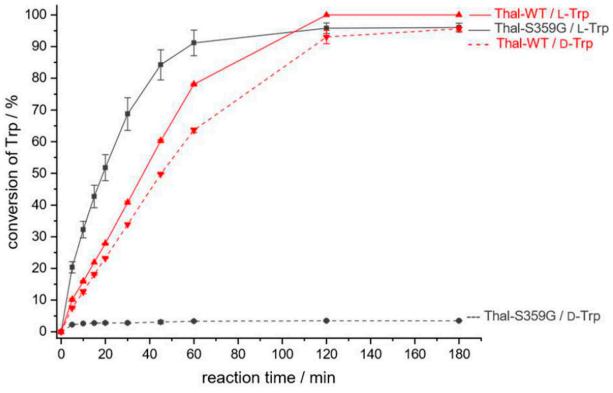

Figure 6. Thal-WT and Thal-S359G catalyzed bromination of D- or L-Trp. Thal-S359G showed highest conversion of the L-enantiomer whereas negligible bromination is noted for the D-enantiomer. Thal-WT exhibits comparable conversion of both L- and D-Trp, with a slight preference for the native L-enantiomer. Reaction conditions: 7 μM Thal variant, 1 mM D-Trp or L-Trp, cofactor regeneration, 25 °C.

The Active-Site Ser Residue Plays a Crucial Role in Enantiomer Selectivity

As these previous findings underline the peculiar role of the active site mutation, we questioned whether the advantages of S359G mutation are also applicable to related halogenases. Thus, the corresponding point mutants were generated in RebH and PyrH, respectively (RebH-S358G/PyrH-S355G). In contrast to the observations made for Thal-S359G, the RebH and PyrH mutants did not reveal a significant increase in performance. Even though RebH-S358G exhibited 23% elevated activity compared to the WT at 25 °C, this effect was not observed at 40 °C and not as pronounced as for the Thal-S359G variant. Introduction of the mutation in PyrH completely abolished its activity (Figure 7A). Moreover, these active site variants were even detrimental on the thermostability of both halogenases (Table S3). To deepen the study of the catalytic role of S359 the corresponding Ala mutants were generated in accordance to an analogous PrnA mutant previously reported by van Pée *et al.*[54] As site-saturation mutagenesis of Thal-GRV confirmed Gly as the most beneficial amino acid, the corresponding mutant Thal-S359A was therefore of minor interest. RebH-S358A and PyrH-S355A exhibited lower performance than the WT with regard to activity and thermostability (Figure 7A, Table S3). To conclude, the beneficial effects on activity and thermostability observed for Gly359 are specific for the 6-halogenase Thal whereas they are not valid for other FAD-dependent halogenases such as its close homologue RebH. However, similar to the Thal-S359G variant, the RebH-S358G mutant displayed a significantly reduced conversion of D-Trp, dropping from 97% (WT) to merely 14% (Figure 7B). Obviously, this observation is consistent among the halogenases tested herein. This consistency provides evidence that this position is decisive for substrate selectivity. The mutation to Ala did not alter enantiomer selectivity merely reducing the overall activity of RebH.

Clearly, Ser influences enantiomer selectivity which is rather surprising as this residue is oriented proximally to the indole moiety and undergoes no direct interactions to the amino acid backbone (Figure 3). Noteworthy, the neighboring residue Glu346 supports positioning of the substrate tryptophan by a hydrogen bond between the NH group of the indole ring and the carbonyl group of peptide bond between Glu346 and Ser347.[45,54] Recently, desymmetrization of prochiral methylene dianilines by a RebH mutant was demonstrated by Lewis *et al.*, providing an example of engineering the enantioselectivity of a flavin-dependent halogenase.[56] In our study, alteration of one residue within the active site allows for a tremendous influence on L-/D-selectivity and we were able to alter specificity of the substrate enantiomer. This points to an unexpected crucial role of Ser in substrate recognition presumably attractive for engineering of halogenase specificity.

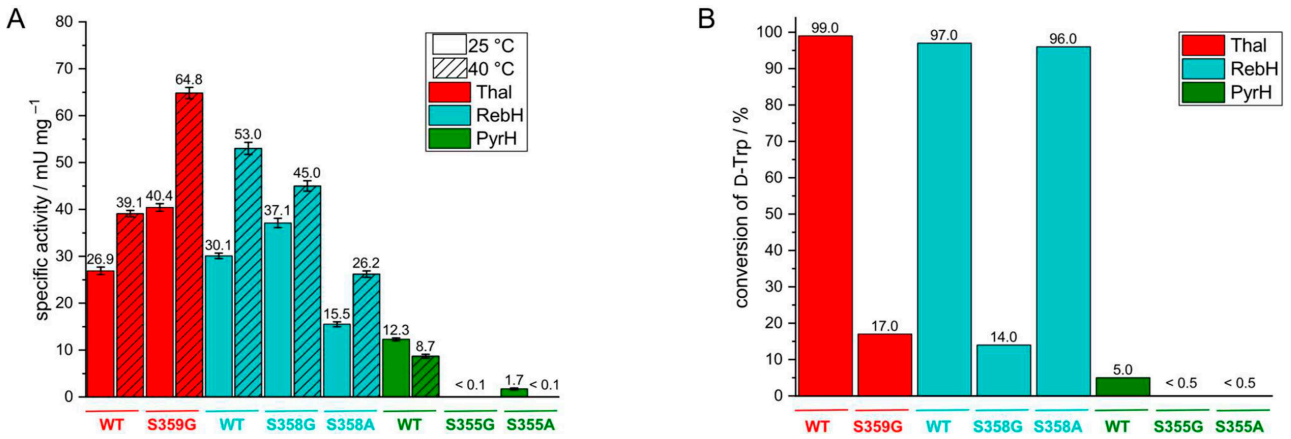

Figure 7. Impact of the active site Ser residue on activity and enantioselectivity of the halogenases Thal, RebH and PyrH. A) Determination of specific activity at 25 °C and 40 °C revealed elevated activity of the Thal mutant whereas a mutation to Gly in RebH or PyrH did not significantly improve activity. B) The conversion assay of D-Trp to D-6-Br-Trp resulted in significantly reduced performance of mutants indicating higher enantiospecificity as a result of the mentioned amino acid exchange.

Conclusions

Halogenase stability often cannot be increased without affecting conformational flexibility as a crucial factor lowering enzyme activity. This observation is ascribed to a stability-activity trade-off typically occurring for engineered enzymes. Therefore, a balance between stabilization and maintenance of activity is essential to encounter the requirements for biocatalysis.[57,58] A combination of different evolution strategies including directed evolution, rational design as well as site-saturation mutagenesis was employed aiming to the development of a significantly more thermostable halogenase with elevated activity. Seven different residues were identified in the tryptophan 6-halogenase Thal and their impact on thermostability and activity was analyzed in detail. Thal-GLV displays significantly increased thermostability compared to Thal WT ($\triangle T_{50} = 16.0$ K; $\triangle T_M = 23.5$ K) and strongly elevated enzyme activity at 25 °C. Moreover, the single mutation K374W turned out to strongly enhance overall halogenation efficiency at 25 °C. We were able to identify beneficial residues within the protein scaffold (amino acid position 359, 374 and 393) that contribute to thermostability as well as elevated activity. Interestingly, hydrophobic interactions located at the interface between the Thal monomers were favorable for improved thermostability. MS analysis of selected Thal mutants indicates an enhanced tendency for dimer formation compared to the WT. These results suggest that dimerization occurs as a beneficial factor for halogenase stabilization essential to an enhanced synthetic utility. The mutation S359G tremendously increases thermostability and activity despite its location within the active site. Similar effects of this mutation could not be observed for related tryptophan halogenases. Noteworthy, this mutation also increases enantiomer selectivity giving significantly reduced conversion of D-Trp. The results shown herein underscore that halogenases, promising tools for enzymatic C–H activation, can be improved by random or rational evolution strategies. This evolution campaign also opens up novel motifs having a strong influence on fundamental enzyme properties. Thermostable and more active Thal variants obtained herein will find their way into chemoenzymatic synthesis for efficient production of haloarenes. Based on these findings novel halogenases with altered substrate spectrum and high robustness may be developed that further expand the scope of enzymatic halogenation.

Experimental Section

Analytics

Reversed Phase-High Performance Liquid Chromatography (RP-HPLC)

A Shimadzu CBM-20A chromatography system was employed for analytical measurements equipped with a diode array detector SPD-M20A IVDD (Shimadzu), pump Nexera XR liquid chromatography LC-20AD$_{XR}$ (Shimadzu), column oven CTO-20A (Shimadzu) and an autosampler Nexera XR SIL-20A$_{xr}$ (Shimadzu). For separation a Luna 3 µM C_{18} column 100 Å, 100×2 mm from Phenomenex with a flow rate of 0.65 mL min^{-1} was used. Absorbance was measured simultaneously at 220, 254 and 280 nm. Eluents: A: water/trifluoroacetic acid (99.9:0.1), B: acetonitrile/trifluoroacetic acid (99.9:0.1). Elution profile at 40 °C column temperature: (A %): 0–5.5 min: linear gradient from 95 % to 5 %, 5.5–6 min: 5 %, 6–6.1 min: gradient from 5 % to 95 %, 6.1–9.0 min: 95 %.

High-Performance Liquid Chromatography-Mass Spectrometry (LC-MS)

Separation was performed with a 1200 HPLC system consisting of an autosampler, degasser, binary pump, column oven and diode array detector (Agilent Technologies, Santa Clara, CA, USA) using a C_{18} Hypersil Gold column, 3 µm, 150×2.1 mm (Thermo Scientific) and solvent flow was directly introduced to ESI-*oa*-ToF (orthogonal acceleration time-of-flight) mass spectrometer. ESI mass spectra were acquired employing an Agilent 6220 time-of-flight mass spectrometer from Agilent Technologies (Santa Clara, CA, USA) in

extended dynamic range mode containing a Dual-ESI source, operating with a nitrogen generator NGM 11. The mass axis was externally calibrated with ESI-L Tuning Mix (Agilent Technologies, Santa Clara, CA, USA) as calibration standard. HPLC solvent A: water/acetonitrile/formic acid (94.9:5:0.1); HPLC solvent B: water/acetonitrile/formic acid (5:94.9:0.1). Gradient elution: (A%): 0–10 min gradient from 98% to 2%, 10–11 min: 2% isocratic, 11–11.5 min: gradient from 2% to 100%, 11.5–15 min: 100%) with a flow rate of 0.3 mL min^{-1} and column temperature of 40 °C.

Protein Analysis Using Nano-Electrospray Ionization-Mass Spectrometry (Nano-ESI-MS)

His_6-tagged halogenase was purified via HisTalon affinity chromatography, dialyzed against 100 mM ammonium acetate buffer, pH 7.0 and applied for nano-ESI-MS measurements under native conditions (final concentration: 10 μM). Under denaturing conditions, his_6-tagged halogenase (final concentration 10 μM) was dissolved in 50% MeCN, 0.1% formic acid. Nano-ESI measurements were performed using a Q-IMS-*oa*-TOF mass spectrometer Synapt G2Si (Waters GmbH, Manchester, UK) in resolution mode, interfaced to a nano-ESI ion source. Nitrogen served both as the nebulizer gas and the dry gas for nano-ESI. Nitrogen was generated by a nitrogen generator NGM 11. Samples were dissolved in ammonium acetate buffer (100 mM, pH 7.0) and introduced by static nano-ESI using *in-house* pulled glass emitters. The mass axis was externally calibrated with ESI-L Tuning Mix (Agilent Technologies) as calibration standard. Scan accumulation and data processing was performed with MassLynx 4.1 (Waters GmbH, Manchester, UK) on a PC Workstation. The spectra shown here were generated by the accumulation and averaging of several single spectra. Determination of protein masses was performed using centroided data using the ESIprot software.[59]

General Procedures

Standard chemicals and solvents were obtained from commercial suppliers in highest purity suitable for analytical applications (p. a.). Restriction enzymes were purchased from New England Biolabs, DNA polymerase was supplied from Roboklon and Random Mutagenesis GeneMorph II Kit obtained from Agilent.

Molecular Cloning

Molecular biology was performed according to standard procedures as described.[60] Codon-optimized gene for *E. coli* encoding Thal (Uniprot ID: A1E280), RebH (Uniprot ID: Q8KHZ8) or PyrH (Uniprot ID: A4D0H5) was subcloned into pET28a as reported earlier and employed for heterologous expression in *E. coli* BL21 (DE3) pGro7.[18] The plasmid vector pET21-ADH encoding alcohol dehydrogenase was kindly supplied from Prof. Dr. Werner Hummel, Bielefeld University, and pCIBhis-PrnF encoding the flavin reductase was donated by Prof. Dr. Karl-Heinz van Pée, TU Dresden. Plasmid pGro7 was purchased from TaKaRa. *E. coli* DH5α and BL21(DE3) were purchased from Novagen.

Heterologous Expression in *E. coli*

Flavin Reductase PrnF and Alcohol Dehydrogenase RR-*ADH*

Expression of PrnF and alcohol dehydrogenase was conducted according to our already published procedure.[11]

Halogenase Thal, RebH, PyrH and Respective Variants

1.5 L LB medium containing kanamycin (60 mg L^{-1}) and chloramphenicol (50 mg L^{-1}) was inoculated with 20 mL L^{-1} overnight culture of *E. coli* BL21 (DE3) pGro7 pET28a-Thal, pET28a-RebH, pET28a-PyrH or its respective variants. The expression culture was incubated at 37 °C until an $OD_{600} = 0.6$ was reached. Temperature was decreased to 25 °C for 30 min and overexpression subsequently induced by addition of 0.1 mM IPTG and 2 g L^{-1} L-arabinose. Cells were shaken at 150 rpm for 20 h, harvested by centrifugation (3220×g, 30 min, 4 °C), washed with 40 mL Na_2HPO_4 buffer (0.1 M, pH 7.4) and stored at −20 °C.

Determination of Flavin Reductase activity at 25 °C and 40 °C

Determination of PrnF activity was performed according to our already published procedure including the following modifications.[11] The volumetric activity of the elution fractions of the flavin reductase PrnF from *Pseudomonas fluorescens* was determined as triplicates by monitoring the decrease of absorption at λ = 340 nm due to the oxidation of $NADH + H^+$ to NAD^+ (ε = 6.3 mL μmol^{-1} cm^{-1}) in a final volume of 1 mL containing 20 μL of diluted flavin reductase (dilution 1:100), 10 mM Na_2HPO_4 pH 7.4, 50 μM FAD and 160 μM NADH. All components were pre-equilibrated at 25 °C/40 °C for 30 min. Afterwards pre-equilibrated PrnF was added to residual components and the conversion rate of the substrate was determined using a UV-3100 PC spectrometer (VWR) by regression of the linear range (15 s after addition of the enzyme).

Determination of Alcohol Dehydrogenase Activity

Activity determination of *RR*-ADH from *Rhodococcus* spp. was performed as previously published.[11]

Protein Purification

His_6-tagged fusion protein was extracted from *E. coli* cells after expression by resuspending bacteria in 40 mL 50 mM Na_2HPO_4 pH 7.4, 300 mM NaCl for subsequent lysis by French Press (3×). Cell debris was removed by centrifugation (10000×g, 30 min, 4 °C) and the supernatant filtered through 0.45 μm Whatman filter. The cleared lysate was loaded on HisTALON agarose affinity resin (bed volume of 1.5 mL resin), incubated for 1 h at 4 °C to enable protein binding, followed by two washing steps adding 10 mL 50 mM Na_2HPO_4 pH 7.4, 300 mM NaCl and afterwards 50 mM Na_2HPO_4 pH 7.4, 300 mM NaCl, 10 mM imidazole. The fusion protein was isolated by addition of 300 mM NaCl, 300 mM imidazole, 50 mM Na_2HPO_4 pH 7.4. Fractions of 0.5 mL were collected and protein concentration was determined by Nano-Drop UV spectroscopy. For following enzyme characterization the protein was dialyzed against 15 mM Na_2HPO_4, 30 mM NaBr, pH 7.4 (5 L reservoir) overnight to remove contaminating chloride ions.

Directed Evolution of Tryptophan 6-Halogenase Thal

Generation of Megaprimers (epPCR)

Construction of mutant libraries was performed based on the already described procedure by Weiß *et al.*[61] For error-prone PCR libraries, the genes encoding the respective variants of Thal were amplified by applying the GeneMorph II Random Mutagenesis Kit (Agilent Technologies) using the following primers: pET28a-NdeI-FW and pET28a-BamHI-Stop-RV (Table S1). 50 ng of parental

plasmid template (1st round of evolution: pET28-Thal-GR, 2nd round of evolution: pET28-Thal-GRV) was employed in a total volume of 50 μL and amplified over 30 cycles of mutagenesis as follows: (a) 95 °C, 2 min; (b) 30 cycles: 95 °C, 30 s; 55 °C, 30 s; 72 °C, 90 s; (c) 72 °C, 10 min. Three randomly selected colonies were sent for sequencing and revealed an average mutation frequency of three nucleotide exchanges per gene. PCR products were purified according to the manual instructions using the NucleoSpin Gel and PCR Clean-up Kit (Macherey & Nagel). The sample was eluted in 25 μL for use as megaprimers in the following MEGAWHOP-PCR.[62]

Performance of MEGAWHOP (Whole-Plasmid PCR)

Mutated halogenase genes were inserted into plasmid vector by making use of MEGAWHOP according to the following procedure in a total volume of 50 μL: Pfu-buffer, 0.8 mM dNTPs, 75 ng parental plasmid (pET28-Thal-GR), 6 μL purified megaprimers as described above and 1.0 μL of Pfu Plus! DNA polymerase. The amplification was performed as follows: (a) 94 °C, 2 min; (b) 25 cycles: 94 °C, 25 s; 58.5 °C, 30 s; 72 °C, 7.0 min; (c) 7 °C, 14 min. The PCR product was digested with *Dpn*I (20 U, 2 h at 37 °C) and subsequently the restriction enzyme was inactivated by incubation at 80 °C for 20 min. 5 μL sample volume was directly transformed into a 75 μL aliquot of electro-competent *E. coli* DH5α (2 kV, 5 ms). After transformation, 1 mL SOC medium was added and after 55 min incubation (37 °C, 500 rpm) a sample of 50 μL was plated out on LB agar supplemented with Kan (60 mg L^{-1} kanamycin) and the remaining sample was employed for inoculation of a 50 mL LB-Kan (60 mg L^{-1} kanamycin) overnight culture (37 °C, 150 rpm). After overnight incubation colonies were counted to calculate the number of transformants (5000 transformants were usually obtained). The overnight culture was employed for plasmid isolation and chemo-competent *E. coli* BL21(DE3) pGro7 cells were transformed via heat-shock with 40–80 ng of the library plasmid DNA. After incubation at 37 °C 0.5–1.0 mL was plated out on Kan/Cam plates (60 mg L^{-1} kanamycin, 50 mg L^{-1} chloramphenicol) for Thal library screening as described below.

Library Expression

Library expression, halogenase characterization and screening for increased thermostability based on high-throughput Suzuki-Miyaura cross-coupling was performed with some modifications following our already published procedure.[38] Colonies were picked and arrayed by inoculation of 150 μL LB medium (Kan: 60 mg L^{-1}, Cam: 50 mg L^{-1}) in 96-well plates. Plates were sealed with AeraSeal and grown for 18 h at 30 °C in an orbital shaker (800 rpm, Heidolph Titramax 1000). Deep-well plates containing 1.0 mL TB medium per well supplemented with the appropriate antibiotics was inoculated with 50 μL precultures and grown at 37 °C, 800 rpm. After 3 h temperature was decreased to 25 °C and plates were incubated for additional 30 min. Protein expression was induced by addition of 0.1 mM IPTG and 2 mg mL^{-1} L-arabinose and shaken for 20 h (1000 rpm) at 25 °C. Cells were harvested by centrifugation (3220× g, 45 min, 4 °C), supernatant was discarded and expression plates were stored at −20 °C.

Cell lysis and Screening for Thermostability

Expression plates were thawed for 20 min on ice and 150 μL lysozyme (2 mg mL^{-1}) as well as 10 μL DNAseI (1 mg mL^{-1}), diluted in bromination buffer (10 mM K_2HPO_4 pH 7.4, 30 mM NaBr) were added to each well. Cell pellets were resuspended and shaken vigorously at 25 °C for 3 h in an orbital shaker. To screen for increased thermostability the microtiter plate was incubated in a water bath at 59 °C for 20 min (1st round) and at 64 °C (2nd round). Afterwards cell debris was removed by centrifugation (3220×g, 30 min, 4 °C). 50 μL thermally treated lysate were used for halogenation at 25 °C by addition of 50 μL bromination buffer containing 5 mM L-tryptophan, 2.5 U mL^{-1} PrnF, 1 U mL^{-1} alcohol dehydrogenase, 10 μM FAD, 1 mM NAD^+, 5% (v/v) *iso*-propanol, 10 mM K_2HPO_4 (pH 7.4), 30 mM NaBr, 0.1 mg mL^{-1} ampicillin and 5 μM PMSF. Plates were sealed with AeraSeal and bromination was conducted at 150 rpm, 25 °C for 20 h. Endpoint conversion was determined by high-throughput Suzuki-Miyaura cross-coupling as described below.

High-Throughput Suzuki-Miyaura cross-Coupling

Subsequent to enzymatic bromination catalyzed by thermally treated Thal variants the assay plates were centrifuged (3220 × g, 10 min, 4 °C) and 10 μL supernatant from each well was transferred into a 96-well PCR plate. Coupling mastermix containing 3-aminophenylboronic acid (6.7 mM) and K_3PO_4 (10 mM) in aqueous solution was prepared. 75 μL mastermix were added to each well with regard to a final concentration of 5 mM boronic acid and 7.5 mM base in a total volume of 100 μL in the coupling assay. Catalyst mastermix consisting of 1.7 mM Na_2PdCl_4 as well as 5 mM sSPhos (sodium 2′-dicyclohexylphosphino-2,6-dimethoxy-1,1′-biphenyl-3-sulfonate hydrate) was pre-activated at 40 °C for 10 min under vigorous shaking. 15 μL Pd catalyst solution was added to each well giving 0.25 mM Na_2PdCl_4 and 0.75 mM sSPhos as end concentration. Plates were sealed with adhesive film and incubated for 2 h at 95 °C in a drying oven. Reaction was quenched by addition of 90 μL 2% TFA added to 15 μL sample per well and fluorescence emission was recorded at 430 nm (excitation: 300 nm) using a microplate reader (Tecan, Infinite M200).

Site-Directed and Site-Saturation Mutagenesis

All Thal, RebH and PyrH variants were prepared following the QuikChange II Site-Directed Mutagenesis Kit with modifications. Primers were designed with the desired mismatches to incorporate the corresponding mutations. For site-saturation mutagenesis, primers with NNK degenerated codon in the position were applied (see Supporting Information, Table S1). The PCR conditions were as follows: 100 ng plasmid DNA as template, 5 μL 10× Pfu-reaction buffer, 200 μM dNTPs, 0.5 μM forward primer, 0.5 μM reverse primer, 2.5 U/μl Pfu-Plus! polymerase. PCR was performed in a volume of 50 μL by applying the following procedure: 95 °C 120 s, (95 °C 30 s, 58 °C 30 s, 68 °C 7.5 min) for 25 cycles, 68 °C 7 min. Amplification was verified by agarose gel electrophoresis and the resulting amplificate was directly digested with *Dpn*I by adding 20 U to each amplification reaction. The digestion was conducted at 37 °C for 2 h and the enzyme subsequently inactivated at 80 °C for 20 min. The mixture was purified using QIAquick PCR Purification Kit (Qiagen), 10 μL of DNA solution was transformed via heat shock into chemocompetent *E. coli* DH5α, plated on LB agar supplemented with appropriate antibiotics (kanamycin) and grown overnight at 37 °C. For plasmid isolation 10 mL LB medium containing the appropriate antibiotic (kanamycin, 60 mg L^{-1}) was inoculated with an individual colony and cells were grown at 37 °C overnight. Plasmids were purified using QIAprep Spin miniprep Kit (Qiagen) according to the manufacturer's instructions. After confirmation of codon distribution in the case of a site-saturation mutagenesis or sequence verification of point mutants (sequencing performed via GATC Biotech), the plasmids were transformed into chemocompetent *E. coli* BL21(DE3) pGro7 cells for halogenase expression.

Biocatalytic Halogenation Assays

Determination of Melting Temperature (T_M) for Thal, RebH, PyrH and Respective Variants

The melting temperature (T_M) of Thal-WT, RebH-WT, PyrH-WT and evolved variants (8 μM) was evaluated employing a nanoDSF device (Prometheus NT.48, NanoTemper Technologies GmbH). Capillaries were filled from respective solutions (10 μL). Samples were measured in the Prometheus NT.48 in a temperature range of 20–95 °C. Data analysis was performed using NT Melting Control software (NanoTemper Technologies GmbH). The T_M was determined by fitting the tryptophan fluorescence emission ratio of 350 nm to 330 nm using a polynomial function, in which the maximum slope is indicated by the peak of its first derivative.

Temperature-Conversion Gradient for T_{50} Determination of Thal Variants

A stock solution of Thal or corresponding variants (145 μM) in 15 mM Na_2HPO_4 pH 7.4 and 30 mM NaBr) was pipetted as triplicate into a 96-well PCR plate (60 μL per well) and incubated in a thermocycler (Peqlab, Primus 96 advanced) using a gradient from 42.0–75.0 °C for 20 min. After centrifugation (4000×g, 10 min, 4 °C) 40 μL of each sample (40 μM final halogenase concentration) was applied to determine residual halogenase activity and employed in a 150 μL reaction mixture containing 5 mM L-tryptophan, 2.5 U mL^{-1} flavin reductase PrnF, 1 U mL^{-1} alcohol dehydrogenase, 10 μM FAD, 1 mM NAD^+, 10 mM K_2HPO_4 pH 7.4, 30 mM NaBr and 5% *iso*-propanol in a 96-well plate. The plate was sealed with AeraSeal and shaken at 150 rpm and 25 °C. After 20 h, final conversion of Trp was determined via RP-HPLC, plotted against temperature and half-maximal conversion (T_{50}) was calculated from sigmoidal regression.

Determination of Specific Activity for Thal, RebH, PyrH and Variants

The calculation of the specific activity referred to the conversion of 1 mM L-tryptophan at 25 °C or 40 °C in presence of concomitant cofactor regeneration. In a total volume of 750 μL, 1 mM substrate L-tryptophan, 2.5 U mL^{-1} PrnF, 1 U mL^{-1} ADH, 10 μM FAD, 1 mM NAD^+, 15 mM Na_2HPO_4 pH 7.4, 30 mM NaBr and 5% *iso*-propanol were combined in 96-deep well plates. The mixture was pre-equilibrated at 25 °C or 40 °C for 10 min and finally the reaction was initiated by addition of tryptophan halogenase dissolved in 15 mM Na_2HPO_4, pH 7.4, 30 mM NaBr in a final concentration of 7 μM. During incubation at 25 °C/40 °C, 600 rpm, in intervals of 5–10 min a 50 μL aliquot was taken and inactivated by addition of an equal volume of methanol. The resulting samples were centrifuged (5 min, 4000×g) and 80 μL supernatant transferred to a new 96-well plate and diluted with an equal volume of H_2O. To determine the specific activity the formation of Br-Trp was analyzed via analytical RP-HPLC and plotted against reaction progress. The linear phase of the enzyme reaction, usually from 0–30 min, was analyzed by linear regression and the specific activity was calculated accordingly based on the amount of tryptophan halogenase added to the reaction (see Supporting Information, Figure S1, Table S2).

Halogenation of D-Tryptophan Using Purified Thal, RebH, PyrH and Respective Variants

Enzymatic halogenation of D-tryptophan was assayed in a total volume of 200 μL under gentle shaking at 25 °C. Substrate D-tryptophan was added to a final concentration of 1 mM together with 1 mM NAD^+, 0.01 mM FAD, 1 U mL^{-1} *RR*-ADH, 2.5 U mL^{-1} PrnF, 5% (v/v) *iso*-propanol, 10 mM Na_2HPO_4 pH 7.4 and 30 mM NaBr or NaCl. Purified Thal-WT, RebH-WT, PyrH-WT or variants were added to a final concentration of 25 μM. Reactions were performed as duplicate and reaction progress was monitored by analytical RP-HPLC. For this, at different time points aliquots of 50 μL were taken from the reaction mixture and quenched by adding an equal volume of methanol. The mixture was centrifuged (12000×g, 10 min) and the supernatant analyzed via analytical RP-HPLC.

Chlorination of L-Tryptophan Employing Purified Thal-GWV

Enzymatic chlorination was assayed in a total volume of 500 μL under gentle shaking at 25 °C. The substrate L-tryptophan was added to a final concentration of 1 mM together with 1 mM NAD^+, 0.01 mM FAD, 1 U mL^{-1} *RR*-ADH, 2.5 U mL^{-1} PrnF, 5% (v/v) *iso*-propanol, 10 mM Na_2HPO_4 pH 7.4 and 30 mM NaCl. Purified Thal-GWV was added to a final concentration of 80 μM. Reactions were performed as duplicate and after 24 h final conversion was monitored by LC-MS. For this, aliquots of 50 μL were taken from the reaction mixture and quenched by adding an equal volume of methanol. The mixture was centrifuged (12000×g, 10 min) and the supernatant analyzed via LC-MS (see Supporting Information, Figure S8).

Determination of Optimal Reaction Temperature (T_{opt}) for Thal-WT and Thermostable Variants

Enzymatic bromination was assayed in a total volume of 200 μL under gentle shaking at 25 °C, 30 °C, 35 °C and 40 °C. Substrate L-tryptophan was added to a final concentration of 5 mM together with 1 mM NAD^+, 0.01 mM FAD, 1 U mL^{-1} *RR*-ADH, 2.5 U mL^{-1} PrnF, 5% (v/v) *iso*-propanol, 10 mM Na_2HPO_4 pH 7.4 and 30 mM NaBr. Purified Thal-WT, Thal-GR or Thal-GLV was added to a final concentration of 20 μM. Reactions were performed as duplicate at the temperature indicated and after 22 h final conversion was analyzed by analytical RP-HPLC. Conversion-temperature profiles were obtained by plotting conversion of substrate against reaction temperature (see Supporting Information, Figure S2).

Long-Term Stability Assay of Thal-WT and Thal-GLV

Purified tryptophan halogenase (50 μM in 15 mM Na_2HPO_4, pH 7.4 and 30 mM NaBr) was stored at 40 °C in a thermoshaker for several hours. At different time points an aliquot of 10 μL was taken and applied for enzymatic bromination at 25 °C. For this, the sample was mixed with 2 mM L-tryptophan, 2.5 U mL^{-1} PrnF, 1 U mL^{-1} *RR*-ADH, 0.01 mM FAD, 1 mM NAD^+, 5% (v/v) *iso*-propanol, 10 mM Na_2HPO_4 pH 7.4 and 30 mM NaBr in a final volume of 100 μL. Reaction mixtures were incubated for 20 h at 25 °C in a thermoshaker (500 rpm) and afterwards aliquots of 50 μL were taken and quenched by adding an equal volume of methanol. After centrifugation (12000×g, 10 min) the supernatant was analyzed by analytical RP-HPLC. Measurements were performed as duplicate (see Supporting Information, Table S4).

Analysis of Substrate Panel of Thal-WT, Thal-S359G and Thal-GLV

The substrate scope of Thal-WT, Thal-S359G and Thal-GLV was tested for the following substrates: phenol, methyl pyrrole-3-carboxylate, indole and tryptamine. L-Trp served as a positive control. In a total volume of 100 μL, 1 mM substrate, 2.5 U mL^{-1} PrnF, 1 U mL^{-1} *RR*-ADH, 10 μM FAD, 1 mM NAD^+, 15 mM Na_2HPO_4

pH 7.4, 30 mM NaBr and 5% *iso*-propanol were combined in a 96-well plate and purified tryptophan halogenase was added in a final concentration of 80 μM. Reaction mixtures were incubated for 24 h at 25 °C (500 rpm) and the reaction was stopped by adding an equal volume of methanol (100 μL). After centrifugation (4000 × g, 10 min) the supernatant was diluted with an equal volume of water and analyzed by LC-MS. All reactions were performed as duplicate (see Supporting Information, Table S5).

Comparison of Thal-WT and Thal-S359G Catalyzed Bromination of D- and L-Tryptophan

Enzymatic bromination of D- and L-tryptophan was assayed in a total volume of 1 mL under shaking at 25 °C. Substrate D- or L-tryptophan was added to a final concentration of 1 mM together with 1 mM NAD^+, 0.01 mM FAD, 1 U mL^{-1} *RR*-ADH, 2.5 U mL^{-1} PrnF, 5% (*v/v*) *iso*-propanol, 10 mM Na_2HPO_4 pH 7.4 and 30 mM NaBr. Purified Thal-WT or Thal-S359G was added to a final concentration of 7 μM. At different time points aliquots of 50 μL were taken from the reaction mixture and quenched by adding an equal volume of methanol. The mixture was centrifuged (12000 × g) and the supernatant was analyzed via analytical RP-HPLC to determine conversion. All reactions were performed as duplicate. Analysis of enantiomeric percentage was carried out by Marfey's derivatization described below.

Analysis of D-/L-Tryptophan Preference of Thal-WT and Thal-S359G via Marfey's Derivatization of Reaction Mixtures

Enzymatic bromination of a mixture comprising L- and D-tryptophan in a ratio of 1:1 was assayed in a total volume of 1 mL under shaking at 25 °C in 1.5 mL reaction tubes. The mixture of substrate enantiomers was added to a final concentration of 1 mM (0.5 mM each) together with 1 mM NAD^+, 0.01 mM FAD, 1 U mL^{-1} *RR*-ADH, 2.5 U mL^{-1} PrnF, 5% (v/v) *iso*-propanol, 10 mM Na_2HPO_4 pH 7.4 and 30 mM NaBr. Purified Thal-WT or Thal-S359G were added to a final concentration of 7 μM. Reactions were performed as duplicate and final conversion was monitored by analytical RP-HPLC. Marfey's derivatization of reaction mixtures using N_α-(2,4-dinitro-5-fluorophenyl)-L-alaninamide (FDAA) combined with LC-MS analysis permitted separation of resulting diastereomers comprising either D-/L- tryptophan or D-/L-6-bromotryptophan to provide insight into altered enantiomer preference. In the resulting LC-MS chromatograms the expected diastereomer signals formed upon coupling with FDAA were identified from the MS spectrum and comparison with authentic standards. Therefore, after a reaction time of 24 h 100 μL reaction sample was mixed with 50 μL 0.1 M aq. $NaHCO_3$ solution and 50 μL FDAA solution (10 mM in acetone) was added. The reaction sample was incubated for 60 min at 40 °C in a thermoshaker to enable diastereomer formation. The reaction was stopped by addition of 50 μL 0.1 M aq. HCl, centrifuged (12000 × g, 10 min) and separated via LC-MS (see Supporting Information, Figure S9).

Acknowledgements

We thank Prof. Dr. Karl-Heinz van Pée for providing the plasmid encoding for the flavin reductase PrnF, as well as Prof. Dr. Werner Hummel for providing the plasmid encoding for the alcohol dehydrogenase. In addition, we are grateful to Pia Ferle and Henrik Terholsen (Bielefeld University) for supporting this project.

Conflict of Interest

The authors declare no conflict of interest.

Keywords: directed evolution · enzyme catalysis · enzyme stability · rational mutagenesis · tryptophan halogenase

[1] U. T. Bornscheuer, G. W. Huisman, R. J. Kazlauskas, S. Lutz, J. C. Moore, K. Robins, *Nature* **2012**, *485*, 185–194.
[2] U. T. Bornscheuer, *Philos. Trans. R. Soc. London Ser. A* **2018**, *376*, 20170063.
[3] H. Renata, Z. J. Wang, F. H. Arnold, *Angew. Chem. Int. Ed.* **2015**, *54*, 3351–3367; *Angew. Chem.* **2015**, *127*, 3408–3426.
[4] F. H. Arnold, *Angew. Chem. Int. Ed.* **2018**, *57*, 4143–4148; *Angew. Chem.* **2018**, *130*, 4212–4218.
[5] M. Z. Hernandes, S. M. T. Cavalcanti, D. R. M. Moreira, W. F. de Azevedo Junior, A. C. L. Leite, *Curr. Drug Targets* **2010**, *11*, 303–314.
[6] P. Jeschke, *Pest Manage. Sci.* **2010**, *66*, 10–27.
[7] G. W. Gribble, *Environ. Chem.* **2015**, *12*, 396–405.
[8] F. H. Vaillancourt, E. Yeh, D. A. Vosburg, S. Garneau-Tsodikova, C. T. Walsh, *Chem. Rev.* **2006**, *106*, 3364–3378.
[9] K. Smith, G. A. El-Hiti, *Curr. Org. Synth.* **2004**, *1*, 253–274.
[10] C. D. Murphy, B. R. Clark, in *Stereoselective Synthesis of Drugs and Natural Products*, John Wiley & Sons, Inc., **2013**.
[11] M. Frese, P. H. Guzowska, H. Voß, N. Sewald, *ChemCatChem* **2014**, *6*, 1270–1276.
[12] S. Keller, T. Wage, K. Hohaus, M. Hölzer, E. Eichhorn, K.-H. van Pée, *Angew. Chem. Int. Ed.* **2000**, *39*, 2300–2302; *Angew. Chem.* **2000**, *112*, 2380–2382.
[13] E. Yeh, S. Garneau, C. T. Walsh, *Proc. Natl. Acad. Sci. USA* **2005**, *102*, 3960–3965.
[14] D. Milbredt, E. P. Patallo, K.-H. van Pée, *ChemBioChem* **2014**, *15*, 1011–1020.
[15] S. Zehner, A. Kotzsch, B. Bister, R. D. Süssmuth, C. Méndez, J. A. Salas, K.-H. van Pée, *Chem. Biol.* **2005**, *12*, 445–452.
[16] J. Latham, E. Brandenburger, S. A. Shepherd, B. R. K. Menon, J. Micklefield, *Chem. Rev.* **2018**, *118*, 232–269.
[17] M. Frese, N. Sewald, *Angew. Chem. Int. Ed.* **2015**, *54*, 298–301; *Angew. Chem.* **2015**, *127*, 302–305.
[18] M. Frese, C. Schnepel, H. Minges, H. Voß, R. Feiner, N. Sewald, *ChemCatChem* **2016**, *8*, 1799–1803.
[19] A. D. Roy, R. J. M. Goss, G. K. Wagner, M. Winn, *Chem. Commun.* **2008**, 4831.
[20] W. Runguphan, S. O'Connor, *Org. Lett.* **2013**, *15*, 2850-2853.
[21] E. Burda, W. Hummel, H. Gröger, *Angew. Chem. Int. Ed.* **2008**, *47*, 9551–9554; *Angew. Chem.* **2008**, *120*, 9693–9696.
[22] H. Sato, W. Hummel, H. Gröger, *Angew. Chem. Int. Ed.* **2015**, *54*, 4488–4492; *Angew. Chem.* **2015**, *127*, 4570–4574.
[23] J. Latham, J.-M. Henry, H. H. Sharif, B. R. K. Menon, S. A. Shepherd, M. F. Greaney, J. Micklefield, *Nat. Commun.* **2016**, *7*, 11873.
[24] S. V. Sharma, X. Tong, C. Pubill-Ulldemolins, C. Cartmell, E. J. A. Bogosyan, E. J. Rackham, E. Marelli, R. B. Hamed, R. J. M. Goss, *Nat. Commun.* **2017**, *8*, 229.
[25] M. C. Andorfer, J. E. Grob, C. E. Hajdin, J. R. Chael, P. Siuti, J. Lilly, K. L. Tan, J. C. Lewis, *ACS Catal.* **2017**, *7*, 1897–1904.
[26] M. C. Andorfer, H. J. Park, J. Vergara-Coll, J. C. Lewis, *Chem. Sci.* **2016**, *7*, 3720–3729.
[27] A. Lang, S. Polnick, T. Nicke, P. William, E. P. Patallo, J. H. Naismith, K.-H. van Pée, *Angew. Chem. Int. Ed.* **2011**, *50*, 2951–2953; *Angew. Chem.* **2011**, *123*, 3007–3010.
[28] A.-C. Moritzer, H. Minges, T. Prior, M. Frese, N. Sewald, H. H. Niemann, *J. Biol. Chem.* **2019**, *294*, 2529–2542.
[29] Y. Koyama, M. Hidaka, M. Nishimoto, M. Kitaoka, *Protein Eng. Des. Sel.* **2013**, *26*, 755–761.
[30] I. Wu, F. H. Arnold, *Biotechnol. Bioeng.* **2013**, *110*, 1874–1883.
[31] H. Zhao, F. H. Arnold, *Protein Eng. Des. Sel.* **1999**, *12*, 47–53.
[32] F. H. Arnold, A. A. Volkov, *Curr. Opin. Chem. Biol.* **1999**, *3*, 54–59.
[33] B. K. Shoichet, W. A. Baase, R. Kuroki, B. W. Matthews, *Proc. Mont. Acad. Sci.* **1995**, *92*, 452–456.

[34] Y.-W. Kim, J.-H. Choi, J.-W. Kim, C. Park, J.-W. Kim, H. Cha, S.-B. Lee, B.-H. Oh, T.-W. Moon, K.-H. Park, *Appl. Environ. Microbiol.* **2003**, *69*, 4866–4874.
[35] D. E. Stephens, K. Rumbold, K. Permaul, B. A. Prior, S. Singh, *J. Biotechnol.* **2006**, *127*, 348–354.
[36] C. B. Poor, M. C. Andorfer, J. C. Lewis, *ChemBioChem* **2014**, *15*, 1286–1289.
[37] J. D. Bloom, S. T. Labthavikul, C. R. Otey, F. H. Arnold, *Proc. Natl. Acad. Sci. USA* **2006**, *103*, 5869–5874.
[38] C. Schnepel, H. Minges, M. Frese, N. Sewald, *Angew. Chem. Int. Ed.* **2016**, *55*, 14159–14163; *Angew. Chem.* **2016**, *128*, 14365–14369.
[39] A. D. Bosley, M. Ostermeier, *Biomol. Eng.* **2005**, *22*, 57–61.
[40] M. T. Reetz, J. D. Carballeira, *Nat. Protoc.* **2007**, *2*, 891–903.
[41] W.-N. Niu, Z.-P. Li, D.-W. Zhang, M.-R. Yu, T.-W. Tan, *J. Mol. Catal. B* **2006**, *43*, 33–39.
[42] K. Miyazaki, P. L. Wintrode, R. A. Grayling, D. N. Rubingh, F. H. Arnold, *J. Mol. Biol.* **2000**, *297*, 1015–1026.
[43] *The PyMOL Molecular Graphics System*, version 2.0 Schrödinger, LLC.
[44] D. R. Lide, *CRC Handbook of Chemistry and Physics, 88th ed., J. Am. Chem. Soc.* **2008**, *130*, p. 382.
[45] C. Dong, S. Flecks, S. Unversucht, C. Haupt, K.-H. van Pée, J. H. Naismith, *Science* **2005**, *309*, 2216–2219.
[46] A. S. Panja, B. Bandopadhyay, S. Maiti, *PLoS One* **2015**, *10*, e0131495.
[47] A. C. Leney, A. J. R. Heck, *J. Am. Soc. Mass Spectrom.* **2017**, *28*, 5–13.
[48] K. Root, Y. Wittwer, K. Barylyuk, U. Anders, R. Zenobi, *J. Am. Soc. Mass Spectrom.* **2017**, *28*, 1863–1875.
[49] B. T. Ruotolo, K. Giles, I. Campuzano, A. M. Sandercock, R. H. Bateman, C. V. Robinson, *Science* **2005**, *310*, 1658–1661.
[50] M. M. E. Huijbers, J. W. Wu, A. H. Westphal, W. J. H. van Berkel, *Biotechnol. J.* **2019**, *14*, 1800540.
[51] X. Zhu, W. De Laurentis, K. Leang, J. Herrmann, K. Ihlefeld, K.-H. van Pée, J. H. Naismith, *J. Mol. Biol.* **2009**, *391*, 74–85.
[52] E. Yeh, L. C. Blasiak, A. Koglin, C. L. Drennan, C. T. Walsh, *Biochemistry* **2007**, *46*, 1284–1292.
[53] M. C. Andorfer, J. C. Lewis, *Annu. Rev. Biochem.* **2018**, *87*, 159–185.
[54] S. Flecks, E. P. Patallo, X. Zhu, A. J. Ernyei, G. Seifert, Alexander, C. Dong, J. H. Naismith, K.-H. van Pée, *Angew. Chem. Int. Ed.* **2008**, *47*, 9533–9536; *Angew. Chem.* **2008**, *120*, 9676–9679.
[55] P. R. Neubauer, C. Widmann, D. Wibberg, L. Schröder, M. Frese, T. Kottke, J. Kalinowski, H. H. Niemann, N. Sewald, *PLoS One* **2018**, *13*, e0196797.
[56] J. T. Payne, P. H. Butkovich, Y. Gu, K. N. Kunze, H. J. Park, D.-S. Wang, J. C. Lewis, *J. Am. Chem. Soc.* **2018**, *140*, 546–549.
[57] R. M. Daniel, R. V. Eckert, J. F. Holden, J. Truter, D. A. Crowan, in *Subseafloor Biosphere Mid-Ocean Ridges*, American Geophysical Union, **2013**, pp. 25–39.
[58] R. M. Daniel, D. A. Cowan, *Cell. Mol. Life Sci.* **2000**, *57*, 250–264.
[59] R. Winkler, *Rapid Commun. Mass Spectrom.* **2010**, *24*, 285–294.
[60] J. F. Sambrook, D. W. Russel, *Molecular Cloning: A Laboratory Manual, 3rd ed.*, Cold Spring Harbor Laboratory Press, **2001**.
[61] M. S. Weiß, I. V. Pavlidis, P. Spurr, S. P. Hanlon, B. Wirz, H. Iding, U. T. Bornscheuer, *Org. Biomol. Chem.* **2016**, *14*, 10249–10254.
[62] K. Miyazaki, in *Methods Enzymol.* (Ed.: C. Voigt), Academic Press, **2011**, pp. 399–406.

Manuscript received: September 26, 2019
Accepted manuscript online: October 23, 2019
Version of record online: December 13, 2019